Mat. Res. Soc. Symp. Proc. Vol. 703 © 2002 Materials Research Society V2.6

Nano-Cylinder Structure Studied by X-ray Diffraction

Gu Xu, Zhechuan Feng,[1] Zoran Popovic,[2] Jianyi Lin[3] and Jagadese.J. Vittal[4]
Department of Materials Sci. & Eng., McMaster University, Hamilton, L8S 4L7, Canada
[1]Axcel Photonics Inc., 45 Bartlett Street, Marlborough, Massachusetts, 01752
[2]Xerox Research Center of Canada, Mississauga, Ontario, L5K 2L1, Canada
[3]Department of Physics, National University of Singapore, 119260, Singapore
[4]Department of Chemistry, National University of Singapore, 119260, Singapore

ABSTRACT

The study of nano-cylinder structure has attracted much attention due to the application of multi-wall carbon nanotubes (MWCNTs). While some TEM observations indicate that they are formed by seamless concentric cylinders, other TEM and high pressure X-ray diffraction studies suggest that they look like scrolls of graphite sheets. Although many people now accept the concentric cylinder model, there has been no confirmation reported. On the other hand, this structural difference of MWCNTs plays a crucial role in determining the properties and suitability for future applications. For example, the periodical boundary condition can only be imposed for cylinders, but not for scrolls. To resolve this issue, we employed high-resolution X-ray diffraction to measure detailed profiles of the Bragg peaks for high-purity MWCNTs. We then identified some unusual observations unique to the nano-cylinder structure, followed by the analysis of the structural difference in the Fourier transform between nanotubes formed by scrolls and concentric cylinders. The simulation results are then compared with the experimental data to reveal the structural details.

INTRODUCTION

The determination of nano-sized structures has been a great challenge to materials scientists and engineers. As a recent example, the cylindrical nature of multi-wall carbon nanotubes (MWCNT) has been much debatable [1-11]. While most of the transmission electron microscopy (TEM) observations indicate that they are formed by seamless concentric cylinders [1,2], some TEM and high-pressure X-ray diffraction studies suggest that they look like scrolls of graphite sheets [10,11]. This structural difference of MWCNT plays a crucial role in determining the properties and suitability for future applications, because, e.g., the periodical boundary condition can only be imposed for cylinders, but not for scrolls [12,13]. Although many people accept the concentric cylinder model, there has been no confirmation reported. To resolve this issue, we present high resolution x-ray diffraction results of high purity MWCNT made by catalytic decomposition, where non-equal Bragg peak breaths and shifting of the peak positions were observed. We then identify some unusual observations unique to the nano-cylinder structure, followed by the analysis of the structural difference in the Fourier transform between nanotubes formed by scrolls and concentric cylinders. The simulation results are then compared with the experimental data to reveal the structural details.

EXPERIMENTAL

The x-ray diffraction intensities of carbon nanotube samples were recorded on a Philips X'Pert-MRD Diffractometer with an instrumental broadening of <0.003°/2θ (about 12 arc second) using Cu $K\alpha_1$ radiation (λ=0.15406nm). High purity carbon nanotube samples were prepared by catalytic decomposition of CO using Ni-MgO as the catalyst [14]. This method allows for a good control of the product and over 95% purity [15]. TEM studies show that they have a fairly uniform outer diameter of 20-30nm, each containing about 15 layers of carbon sheets, and extending up to 10 μm in length [14,15]. The resulting θ–2θ scan from 10-100°/2θ is shown in Fig.1a, which was indexed according to graphite structure, with (hk0) representing the reciprocal space of a graphitic layer, and (00l) for the stacking of the layers [11]. Local enlargements of (002) and (004) Bragg peaks are plotted in Fig.1b (taken by 5 min/step).

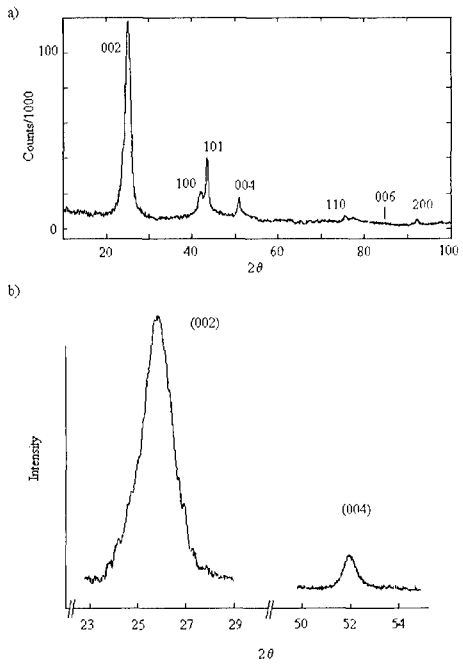

Figure 1. High resolution x-ray diffraction data (θ–2θ scans) of multi-wall carbon nanotubes; a) the entire data set (with Si peaks removed); b) enlargements of (002) and (004) Bragg peaks ($k=4\pi\sin\theta/\lambda$).

RESULTS AND DISCUSSION

From the data, two unusual observations can be made. First of all, the full width at half maximum (FWHM) for the 1st Bragg peak is about 1.45°/2θ, and for the 2nd peak 0.65°/2θ. This produces a ratio of 2.23 of the peak breaths in 2θ, and a ratio of 2.42 in wave vector k ($=4\pi\sin\theta/\lambda$). It is quite unusual because the usually the peak width (measured by k) is related to q/N [16], where q is the peak value of k and N is the number of repeats. The other unusual feature is that the two Bragg peak positions are not obeying the integer multiples of wave vector q, 2q. For example, if we take the 2nd Bragg peak position (2θ = 51.96°) to be the 2q, the 1st peak then should be located at 2θ = 25.30°, rather than shown by the data of 2θ = 25.87°. This also rules out the possibility of having two sets of diffraction peaks, one of which is broader and has a very high effective static Debye-Waller factor, such that the 2nd order Bragg peak becomes much weaker than the 1st.

On the other hand, non-equal peak breaths were also observed in the low resolution x-ray diffraction (XRD) data from the existing literature [11, 17-20], and from a recent neutron diffraction experiment [21], where the (004) peaks were found to be wider than (002). Although this could also be attributed to the lattice distortion, it produces a much higher layer number [19]. From the enlargements of neutron diffraction data [21], the same "mismatch" for the peak positions can also be found, where (004) does not sit on 2q but right-shifted. Apart from the fact that the XRD data were collected using both Cu $K\alpha_1$ +$K\alpha_2$ lines, they are mostly based on the samples made by arc evaporation of graphite, rather than catalytic decomposition of CO. In some cases the sample purity was about 60% [19]. Although most of them found no strong (101) peak, due presumably to the expected misalignment between the graphite layers, the works of Pasqualini [20] and Burian et al [21] suggested that it is possible to have lateral correlation. Therefore, it is likely that they exist in the samples of high purity.

NUMERICAL SIMULATION AND CONCLUSIONS

To resolve the exact structure, a numerical analysis is developed next, to compute the diffraction intensity by the nano-cylinders. For the micro-meter long carbon nanotubes intertwined in space, they can be considered as a collection of randomly distributed tubule segments, which are located at $\mathbf{r'}$ (=x',y',z'), and described by cylindrical co-ordinates $\mathbf{r}$=(r,φ,z):

$$I(\mathbf{k}) \propto |\Sigma_R \rho(\mathbf{R})\exp(i\mathbf{kR})|^2 = |\Sigma_{r'}\exp(i\mathbf{kr'})\int_{cy}d\mathbf{r}\rho(\mathbf{r})\exp(i\mathbf{kr})|^2 \qquad (1)$$

where $\mathbf{R} = \mathbf{r} + \mathbf{r'}$, $\mathbf{k} = (k_x,k_y,k_z)$, and the integral is performed within each segment. Because all segments have different orientations, the local co-ordinate axes (e.g., the tube axis z) vary the orientation from segment to segment. Therefore, we can label the integral of segments by F(k,r'), and equation (1) becomes (with * denotes the complex-conjugate):

$$\Sigma_{r'}\Sigma_{r''}F(\mathbf{k},\mathbf{r'})F^*(\mathbf{k},\mathbf{r''})\exp(i\mathbf{k}(\mathbf{r'}-\mathbf{r''})) = \Sigma_{r'}|F(\mathbf{k},\mathbf{r'})|^2 + \Sigma_{r'\neq r''}F(\mathbf{k},\mathbf{r'})F^*(\mathbf{k},\mathbf{r''})\exp(i\mathbf{k}(\mathbf{r'}-\mathbf{r''})) \qquad (2)$$

where r'' is also used for the location of the tube segment. Before the quantitative calculation of F(k,r'), from the work of Saito et al [17], we learn that for the tube segment, the reciprocal space

consists of annular rings and disks centered around the tube axis. Thus F(k,r') is real and the 2nd exp(ik(r'-r")) in equation (2) can be converted into a cosine function. Due to the random orientation and location of the tube segments, the second part of equation (2) will mostly vanish except at the overlap points of two mis-aligned ring sets, which are further modulated by the cosine factor. Thus the resulting intensity will follow the average of $|F(k)|^2$ over all orientations. The annular rings are then extended into spheres in the reciprocal space, to make the diffraction pattern powder-like. This powder-like nature of the sample can easily be verified by the diffraction measurement at various sample orientations, which was also performed in this study where no sample an-isotropy was detected. Therefore, the Bragg peaks can be calculated from the Fourier transform of any cylindrical segment. According to the convention of graphite structure, (00L) are used to denote reciprocal space along the radial direction of the cylinder, thus only the (r, φ) plane is needed in the calculation (Fig.2a,b). Moreover, the original 3D integral can be further reduced to 2D [22].

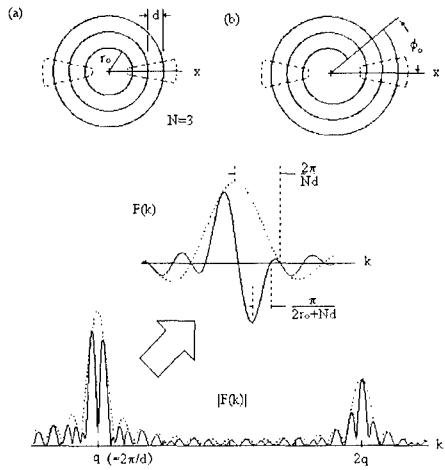

Figure 2. a) Cross-section of multi-wall nanotubes formed by concentric cylinders; b) Cross-section formed by scrolls of graphite sheets; both a) and b) employ polar coordinates r and φ; c) Numerical result of Fourier transform from a), with N=15, r_o=3.3d and F_2=-F_1/2 following equation 1; d) Enlargement of the 1st Bragg peak of c).

As an example, the numerical result of Eq.2 for Fig.2a is shown in Fig.2c. Only two inputs are needed. One is the number of layers, N=15, which can also be estimated from the width of the (002) Bragg peak of the data using Debye Formula [16]. The other is the ratio of F_1/F_2, where F_n being the structure factors for one carbon layer, which forms one repeat unit cell along r-direction. Two Bragg peaks appeared, as indicated by the dashline. The location of the Bragg peak, q, is determined by the periodicity of the repeated structure, d, whereas the overall

peak breadth decided by the number of repeats, N, and the relative peak heights dependent on the choice of F_n. However, since r_o+Nd/2> Nd/2, the period of cos(k(r_o+Nd/2)) is always *smaller* than that of sinc(kNd/2) (Fig.2d). Thus the resulting transform will follow the solid line of Fig.2c, 2d, where the dashlined peak is split into two or more narrower peaks. The above interference will be varied not only by r_o, but also by φ_o for scrolls (Fig.2b). To see this, four representative cases within a cycle have been illustrated by Figs.3a-d. If the nanotube has a scroll form, because φ_o can be arbitrary for each nanotube, the observed diffraction will become the intensity average of the entire cycle. The result is shown in Fig.3e, where the Bragg peak breadths become equal for both q and 2q. This means, the interference has been *averaged out* for scrolls. Due to the discrete nature of r_o ($\propto (n^2+m^2+nm)^{1/2}$, where n,m specify the chiral vector of the inner most cylinder) [23], the intensity average over r_o will *not*, in general, remove the interference effect. For example, when there exists a preferential r_o, and it is chosen to be the value in between Fig.3d and 3a, after the average the result shows that the 2nd peak has only 2/5 the width of the 1st (Fig.3f).

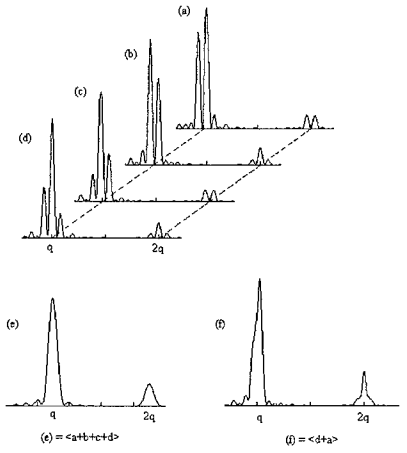

Figure 3. Amplitude square of the Fourier transform of a scroll oriented by φ_o, with N=15, F_2=-F_1/2 and r_o=3.05d; a) $\varphi_o=\pi/4$, b) $\varphi_o=\pi/2$, c) $\varphi_o=3\pi/4$, d) $\varphi_o=\pi$. The same set also serves to illustrate the results for concentric cylinders, which are very similar and without involving φ_o; they represent the changing r_o with: a) r_o= 3.425d, b) r_o=3.30d, c) r_o=3.175d, d) r_o=3.05d; e) Overall $|F(k)|^2$ for scrolls, which has been averaged over the entire cycle of φ_o from 0 to π; f) Example of $|F(k)|^2$ for concentric cylinders, with a small r_o variation between a) and d).

Therefore, the Bragg peak widths (FWHM) must be equal for scrolls, whereas they are, in general, not the same for concentric cylinders (unless the inner radius follows a uniform distribution over a certain range, e.g., several d-spacing). The conclusion can be easily drawn from the comparison of the numerical results and the experimental data, which are in good agreement with Fig.3f for cylinders. In the meantime, it clearly rejects the scroll form (Fig.3e). In

addition to the confirmation of cylinder model, it is interesting to see that the inner tube diameter r_0 does follow a non-uniform distribution for our nanotubes.

To conclude, some unusual diffraction physics was obtained from high resolution x-ray diffraction of high purity MWCNT, in addition to the previous low resolution XRD measurements of low purity samples found in literature. The Fourier analysis not only shows that our multi-wall carbon nanotubes are made of concentric cylinders, but also reveals there is a non-uniform distribution of inner tube diameter. Also, the interference effect discussed in this paper is unique for concentric cylinders because the central canal is separating two identical multiwalls (not only in contrast to scrolls but also in contrast to irregular grains).

REFERENCES

1. S. Iijima, *Nature* **354,** 56 (1991).
2. T.W. Ebbesen and P.M. Ajayan, *Nature* **358,** 220 (1992).
3. A. Thess, R. Lee, P. Nikolaev, H. Dai, P. Petit, J. Robert, C. Xu, Y.H. Lee, S.G. Kim, A.G. Rinzler, D.T. Colbert, G.E. Scuseria, D. Tomanek, J.E. Fischer and R.E. Smalley, *Science* **273,** 483 (1996).
4. M. Ge and K. Sattler, *Science* **260,** 515 (1993).
5. R. Saito, M. Fujita, G. Dresselhaus and M.S. Dresselhaus, *Appl. Phys. Lett.* **60,** 2204 (1992).
6. Z. Zhang and C.M. Lieber, *Appl. Phys. Lett.* **62,** 2792 (1993).
7. J.W.G. Wildoer, L.C. Venema, A.G. Rinzler, R. E. Smalley and C. Dekker, *Nature* **391,** 59 (1998).
8. T. W. Odom, J.L. Huang, P. Kim and C.M. Lieber, *Nature* **391,** 62 (1998).
9. A. Hassanien, M. Tokumoto, Y. Kumazawa, H. Kataura, Y. Maniwa, S. Suzuki and Y. Achiba, *Appl. Phys. Lett.* **73,** 3839 (1998).
10. V.P. Dravid, X. Lin, Y. Wang, X.K. Wang, A. Yee, J.B. Ketterson and R.P.H. Chang, *Science* **259,** 1601 (1993).
11. O. Zhou, R.M. Fleming, D.W. Murphy, C.H. Chen, R.C. Haddon, A.P. Ramirez and S.H. Glarum, *Science* **263,** 1744 (1994).
12. N. Hamada, S. Sawada and A. Oshiyama, *Phys. Rev. Lett.* **68,** 1579 (1992).
13. M.S. Dresselhaus, G. Dresselhaus and R. Saito, *Phys. Rev. B.* **45,** 6234 (1992).
14. P. Chen, H.B. Zhang, G.D. Lin, Q. Hong and K.R. Tsai, *Carbon* **35,** 1495 (1997).
15. P. Chen, X. Wu, J.Y. Lin, H. Li and K.L. Tan, *Carbon* **38,** 139 (2000).
16. B.E. Warren, *X-ray diffraction,* (Addison-Wesley, New York, 1969).
17. Y. Saito, T. Yoshikawa, S. Bandow, M. Tomita and T. Hayashi, *Phys. Rev. B.* **48,** 1907 (1993).
18. S. Bandow, *J. Appl. Phys.* **80,** 1020 (1996).
19. D. Reznik, C.H. Olk, D.A. Neumann and J.R.D. Copley, *Phys. Rev. B.* **52,** 116 (1995).
20. E. Pasqualini, *Phys. Rev. B.* **56,** 7751 (1997).
21. A. Burian, J.C. Dore, H.E. Fischer and J. Sloan, *Phys. Rev. B.* **59,** 1665 (1999).
22. G. Xu, Z.C. Feng, Z. Popovic, J. Lin and J. J. Vittal, *Advanced Materials* **13,** 264 (2001).
23. R. Saito, G. Dresselhaus, and M.S. Dresselhaus, *Physical properties of carbon nanotubes,* (Imperial College Press, London, 1998).